

Improved Robustness and Hyperparameter Selection in Modern Hopfield Networks

Hayden McAlister¹, Anthony Robins¹, Lech Szymanski¹

¹School of Computing, University of Otago, Dunedin, New Zealand.

Abstract

The modern Hopfield network generalizes the classical Hopfield network by allowing for sharper interaction functions. This increases the capacity of the network as an autoassociative memory as nearby learned attractors will not interfere with one another. However, the implementation of the network relies on applying large exponents to the dot product of memory vectors and probe vectors. If the dimension of the data is large the calculation can be very large and result in problems when using floating point numbers in a practical implementation. We describe this problem in detail, modify the original network description to mitigate the problem, and show the modification will not alter the networks' dynamics during update or training. We also show our modification greatly improves hyperparameter selection for the modern Hopfield network, removing hyperparameter dependence on the interaction vertex and resulting in an optimal region of hyperparameters that does not significantly change with the interaction vertex as it does in the original network.

1 Introduction

Autoassociative memories are a class of neural networks that learn to remember states, typically also allowing nearby states to iterate towards similar learned states. These networks act as memories for the learned states, reconstructing lost information and correcting errors in probe states. The Hopfield network (Hopfield, 1982; Hopfield, 1984) is perhaps the most studied model in the class. However, as with all autoassociative memories, the Hopfield network suffers from capacity issues – the number of states that can be stored in a network without error is limited. In the Hopfield network with Hebbian learning, this has been shown to be roughly $0.14N$ for a network of dimension N (McEliece et al., 1987; Hertz, 1991). The modern Hopfield network, also known as the dense associative memory, generalizes the classical Hopfield network by introducing an interaction function parameterized by an interaction vertex (Krotov and Hopfield, 2016; Krotov and Hopfield, 2018). This function controls the range of the influence for learned states, allowing control of the sizes of the attractors and increasing the network capacity. Krotov and Hopfield also introduce several other generalizations which are parameterized by additional hyperparameters. These include hyperparameters corresponding to the learning process such as the initial learning rate, learning rate decay, momentum, learning temperature and the exponent on the error term. Additional hyperparameters were introduced such as the form of the interaction function, the number of memory vectors, and more. In effect, the modern Hopfield network is a potentially more powerful autoassociative memory, but at the cost of increased complexity and reliance on hyperparameter tuning.

We focus on the implementation details of the modern Hopfield network. In particular, we show the exact form given by Krotov and Hopfield suffers from issues relating to computation and numerical stability. The current form calculates the dot product between two vectors of length N then immediately applies a potentially large exponentiation based on the interaction function. This can cause inaccuracies in the floating point numbers used

for computation, or even completely overflow them. In Section 4 we show a modification to the original form – a normalization and shifting of scaling factors – that prevents the computational problems, and prove that the modifications do not change the network behavior for a specific class of interaction functions: homogenous functions. Fortunately, the typical interaction functions – the polynomial interaction function (Equation 5) and rectified polynomial interaction function (Equation 6) – are in this class. In Section 5 we provide experimental results that show our modified network has a stable region of optimal hyperparameters across a wide range of interaction vertices. This is in comparison to the original network which had the optimal hyperparameters shift dramatically as the interaction vertex changed even for the same dataset. We also show that the optimal region of hyperparameters is no longer heavily dependent on the size of the data vectors, meaning applying the modern Hopfield network to a new task will not require massively retuning the hyperparameter selections.

2 Literature Review

Our proposed method of shifting the scaling factors within the interaction function does not appear to have been proposed previously, and other implementations of the modern Hopfield network do not seem to have included it. However, many implementations of the modern Hopfield network use the feed-forward equivalence set forth by Krotov and Hopfield (Krotov and Hopfield, 2016). This equivalence allows the modern Hopfield network to be expressed with some approximations as a feed-forward densely connected neural network with a single hidden layer. This architecture is much easier to implement using traditional deep learning libraries. The feed-forward equivalent model implicitly implements our proposed changes by selecting values of the scaling factor that negate terms arising from a Taylor expansion. This may explain why the feed-forward version of the model is more stable than the auto-associative version.

Normalization is a fairly typical operation in neural networks. In autoassociative memories specifically, we may apply a normalization term to provide a constant power throughout network calculations, which ensures calculations are proportional only to the magnitudes of the learned weights rather than the magnitude of the probe vector. Even more specifically in the Hopfield network this is typically achieved by using binary valued vectors; either over the $\{0, 1\}$ or $\{-1, 1\}$ domain. It has been shown networks using these vectors have the same behavior as networks using graded (continuous value) neurons (Hopfield, 1984). Normalization may also be applied in the learning rule, such as in the Hebbian learning rule, Equation 1 (Hebb, 1949). Normalization in learning may be used to simply scale the weights into something more interpretable, as in the Hebbian, or to achieve a different behavior during training. For example, batch normalization aims to improve training by normalizing the inputs to a layer across a batch – allowing the network to focus only on the variations in training data rather than the potentially overwhelming average signal

(Ioffe and Szegedy, 2015). Layer normalization is another technique that may be used in training to help train recurrent neural networks and remove the dependence on batch size (Ba, Kiros, and Hinton, 2016). However, these techniques are more complex than what we suggest, and tackle problems more general than our proposed changes. Our modifications are not aiming to supersede these techniques in the modern Hopfield network but simply improve network stability and practicality on an implementation level. Moreover, our suggestions do not exclude the possibility of using these other normalization techniques.

Networks related to the modern Hopfield network have employed some normalization techniques in a similar manner to our work. Perhaps most closely related is the continuous, attention-like Hopfield network (Ramsauer et al., 2021) which has shown promising results in the realm of transformer architectures. Ramsauer et al. normalize the similarity scores as we do but work over a slightly different domain: spherical vectors rather than bipolar vectors. While the vector magnitude is still constant, the network has changed rather significantly from the one introduced by Krotov and Hopfield which may slightly change the arguments we make below, although likely not considerably. However, we note that no analysis of the network stability in relation to floating point accuracy is made, and the remainder of our modifications are not applied (e.g. shifting scaling factors inside the interaction function), which our work expands on considerably. Other works have performed a similar normalization, showing there is a trend of applying this technique in network implementation – albeit without noting why it is useful for network stability (Millidge et al., 2022; Liang, Krotov, and Zaki, 2022; Alonso and Krichmar, 2024). Other modern Hopfield applications and derivatives discuss normalization either in a separate context or only tangentially. Extensive work has been done on contrastive normalization (a biologically plausible explanation of network behavior) in the modern Hopfield network and its relation to the restricted Boltzmann machine (Krotov and Hopfield, 2021). Other works employ some of the more advanced normalization techniques, including some we discuss above such as layer normalization by treating the modern Hopfield network as a deep recurrent network (Seidl et al., 2021). Again, these works do not consider shifting the scaling factors within the interaction function.

3 Formalization of the Classical and Modern Hopfield Networks

The classical Hopfield network defines a weight matrix based on the Hebbian of the learned states ξ , indexed by μ :

$$W_{ji} = \sum_{\mu} \xi_j^{\mu} \xi_i^{\mu} \tag{1}$$

The update dynamics for a probe state ζ are defined by the sign of the energy function,

with updates being applied asynchronously across neurons:

$$\begin{aligned}\zeta_i^{(t+1)} &= \text{Sign} \left(\left(W \zeta^{(t)} \right)_i \right) \\ &= \text{Sign} \left(\sum_j W_{ji} \zeta_j^{(t)} \right),\end{aligned}\tag{2}$$

where Sign is the hardlimiting activation function:

$$\text{Sign}(x) = \begin{cases} 1 & \text{if } x \geq 0, \\ -1 & \text{if } x < 0, \end{cases}\tag{3}$$

The modern Hopfield network has significantly different learning rules and update dynamics compared to the classical Hopfield network, as well as major architectural changes such as using a set of memory vectors over an explicit weight matrix. The modern Hopfield network also does away with a simple energy function and instead uses the sign of the “energy difference”:

$$\zeta_i^{(t+1)} = \text{Sign} \left[\sum_{\mu} \left(F_n \left(\xi_i^{\mu} + \sum_{j \neq i} \xi_j^{\mu} \zeta_j^{(t)} \right) - F_n \left(-\xi_i^{\mu} + \sum_{j \neq i} \xi_j^{\mu} \zeta_j^{(t)} \right) \right) \right]\tag{4}$$

Where F_n is the interaction function, parameterized by interaction vertex n . The interaction vertex simply controls how non-linear the interaction function is, usually by increasing the exponent of the interaction function. Typical interaction functions are the polynomial:

$$F_n(x) = x^n,\tag{5}$$

rectified polynomial:

$$F_n(x) = \begin{cases} x^n & \text{if } x \geq 0, \\ 0 & \text{if } x < 0, \end{cases}\tag{6}$$

or leaky rectified polynomial:

$$F_n(x, \epsilon) = \begin{cases} x^n & \text{if } x \geq 0, \\ -\epsilon x & \text{if } x < 0, \end{cases}\tag{7}$$

The classical Hopfield network behavior is recovered when using the polynomial interaction function in Equation 5 and $n = 2$ (Krotov and Hopfield, 2016; Demircigil et al., 2017).

The classical Hopfield network requires only the energy calculation of the current state for updates (Equation 2), while the modern Hopfield network requires the calculation of the energy for the current state when neuron i is clamped on (value 1) and clamped off

(value -1). This is more computationally expensive but allows for updating when the interaction vertex is larger than 2 and the usual arguments for update convergence in the classical Hopfield network fail (Hopfield, 1982; Hopfield and Tank, 1985).

Instead of a weight matrix, the modern Hopfield network uses a set of memory vectors, clamped to have values between -1 and 1 , but not necessarily corresponding to the learned states. Instead, the learned states are used to update the memory vectors in a gradient descent. The loss function used in the gradient descent is strikingly similar to the update rule in Equation 4:

$$L = \sum_a \sum_i (\zeta_{a,i} - C_{a,i})^{2m}$$

$$C_{a,i} = \tanh \left[\beta \sum_{\mu} \left(F_n \left(\xi_i^{\mu} + \sum_{j \neq i} \xi_j^{\mu} \zeta_{a,j}^{(t)} \right) - F_n \left(-\xi_i^{\mu} + \sum_{j \neq i} \xi_j^{\mu} \zeta_{a,j}^{(t)} \right) \right) \right] \quad (8)$$

Where a indexes over the learned states, and i indexes over the neurons. In essence, $C_{a,i}$ is the prediction (bounded between -1 and 1 by \tanh) of neuron i in state ζ_a , so taking $(\zeta_{a,i} - C_{a,i})$ gives an error term we can differentiate to achieve a gradient to optimize with. The new parameters m and β control the learning process. The error exponent m increases the weighting of larger errors, which can help training networks with larger interaction vertices (Krotov and Hopfield, 2016; Krotov and Hopfield, 2018); β scales the argument inside the \tanh function, allowing us to avoid the vanishing gradients of \tanh as the argument grows largely positive or largely negative. Krotov and Hopfield suggest $\beta = \frac{1}{T^n}$, with hyperparameter T representing the network temperature.

Updating by Equation 4 and learning by Equation 8 has been provably very successful. However, we note some issues when implementing the network according to these rules in practice, particularly relating to floating point precision. Inspecting the order in which values are calculated in Equation 4 and 8, first the “similarity score” between a learned state and a memory vector is calculated $(\pm \xi_i^{\mu} + \sum_{j \neq i} \xi_j^{\mu} \zeta_{a,j}^{(t)})$, which is effectively the dot product between two vectors of length N equal to the network dimension. In the worst case, the memory vector could be exactly equal to the learned state, resulting in this dot product having a value of exactly N . For a complex dataset, N could be in the tens of thousands. Next, this similarity score is passed into the interaction function, which will typically have a polynomial-like region such as in Equation 5, 6, or 7. If the worst case is observed, and the interaction vertex n is large (Krotov and Hopfield investigated up to $n = 30$, for example), then we may have to calculate a truly massive number. In the case of $N = 10,000 = 10^4$ and $n = 30$, this value could be up to 10^{120} . Krotov and Hopfield found that for larger interaction vertices, memory vectors tend to approach prototype representations of the data (Krotov and Hopfield, 2016), which makes our worst case *more* likely as the interaction vertex grows. Floating point numbers have only a finite precision (“IEEE Standard for Floating-Point Arithmetic” 2019). In particular, single precision floating point numbers

(“floats”) have a maximum value of around 10^{38} , while double precision floating point numbers (“doubles”) have a maximum value of around 10^{308} . In our example, we are already incapable of even storing the intermediate calculation in a float, and it would not require increasing the network dimension or interaction vertex considerably to break a double either. Furthermore, the precision of these data types grows worse as we approach the limits, potentially leading to numerical instabilities during training or updating. It may seem like we are saved by the next step in the calculation – multiplying by the β term, as we can simply scale the intermediate value back down to something reasonable, but the damage will have already been done and imprecisions or overflow will propagate throughout the calculation. Even in the update rule (Equation 4), where only the sign of the result is relevant, if we encounter a floating point overflow the calculation is undefined.

To fix this, we propose a slight modification to the implementation of the modern Hopfield network. We propose normalizing the similarity score by the network dimension N , bounding it between -1 and 1 rather than $-N$ and N . Additionally, we propose pulling the scaling factor β inside the interaction function, so we can appropriately scale the value before any potential imprecision is introduced by a large exponentiation, making the network more robust. This also allows us to select values of β that are independent of the network dimension – previously, β was the only way to normalize the similarity scores and hence new values of β were required when applying the network to a new task. We show these modifications have the same behavior as the original modern Hopfield network specification in Section 4. In Section 5 we also show by experimentation that these modifications make the network temperature independent of the interaction vertex, something that is not true in the original modern Hopfield network. This makes working with the modern Hopfield network more practical, as it avoids large hyperparameter searches when slightly changing the interaction vertex.

4 Modification and Consistency with Original

Our modifications attempt to rectify the floating point issues by applying a scaling factor to the similarity scores *before* applying the exponentiation of the interaction function. We may then scale the intermediate value down to avoid floating point inaccuracies or errors after exponentiation. To justify our modifications we must show that the scaling factor has no effect on the behavior of the modern Hopfield network in both learning and updates. For the update rule, we will show the sign of the argument to the hardlimiting function in Equation 4 is not affected as we introduce the scaling factor, and move it within the interaction function. For learning, we will make a similar argument about using the scaling factor to shift the argument to the tanh function to a region with reasonable gradient.

4.1 Homogeneity of the Interaction Function

In parts of our proof on the modification of the modern Hopfield network we require the interaction function to have a particular form. We require that value of a function remains the same whether the scaling factor is inside or outside the function (up to scaling the factor):

$$f(ax) = a^k f(x) \forall a > 0 \quad (9)$$

This property is known as homogeneity of the function f , with the exponent k known as the degree of homogeneity. This property is actually stronger than what we require, and interaction functions that are not homogenous may still satisfy our modifications, but we find the proof easier with this stronger property.

We will show that two of the interaction functions of interest are homogenous. The final interaction function, the leaky rectified polynomial interaction function in Equation 7 is not homogenous, but empirically we found this interaction function still behaves under our modifications.

Lemma 4.1.1. *The polynomial interaction function (Equation 5) is homogenous.*

Proof.

$$\begin{aligned} F_n(\alpha x) &= (\alpha x)^n \\ &= \alpha^n x^n \\ &= \alpha^n F_n(x) \end{aligned} \quad (10)$$

Hence, the polynomial interaction function is homogenous, with degree of homogeneity equal to the interaction vertex n . \square

Lemma 4.1.2. *The rectified polynomial interaction function (Equation 6) is homogenous.*

Proof.

$$\begin{aligned} F_n(\alpha x) &= \begin{cases} (\alpha x)^n & \text{if } (\alpha x) \geq 0, \\ 0 & \text{if } (\alpha x) < 0, \end{cases} \\ &= \begin{cases} \alpha^n x^n & \text{if } (\alpha x) \geq 0, \\ 0 & \text{if } (\alpha x) < 0, \end{cases} \\ &= \alpha^n \begin{cases} x^n & \text{if } x \geq 0, \\ 0 & \text{if } x < 0, \end{cases} \\ &= \alpha^n F_n(x) \end{aligned} \quad (11)$$

Note the sign of x is unchanged by scaling by $\alpha > 0$, so we can change the conditions on the limits as we did in Equation 11. Hence, the rectified polynomial interaction function is homogenous, with degree of homogeneity equal to the interaction vertex n . \square

4.2 Update in the Modern Hopfield Network

We start with the right-hand side of Equation 4, introducing an arbitrary constant $\alpha > 0$ to represent any scaling factor we like. We will then show this has no effect on the sign of the result, and we are free to choose $\alpha = \frac{1}{N}$ to normalize the similarity scores by the network dimension.

Theorem 4.2.1. *The behavior of the modern Hopfield network update rule (Equation 4) is unchanged when applying a scaling factor α inside the interaction function. That is:*

$$\begin{aligned} & \text{Sign} \left[\sum_{\mu} \left(F_n \left(\xi_i^{\mu} + \sum_{j \neq i} \xi_j^{\mu} \zeta_j^{(t)} \right) - F_n \left(-\xi_i^{\mu} + \sum_{j \neq i} \xi_j^{\mu} \zeta_j^{(t)} \right) \right) \right] \\ &= \text{Sign} \left[\sum_{\mu} \left(F_n \left(\alpha \left(\xi_i^{\mu} + \sum_{j \neq i} \xi_j^{\mu} \zeta_j^{(t)} \right) \right) - F_n \left(\alpha \left(-\xi_i^{\mu} + \sum_{j \neq i} \xi_j^{\mu} \zeta_j^{(t)} \right) \right) \right) \right] \end{aligned}$$

Proof. The sign of any real number is unaffected by scaling factor $\alpha > 0$:

$$\begin{aligned} & \text{Sign} \left[\sum_{\mu} \left(F_n \left(\xi_i^{\mu} + \sum_{j \neq i} \xi_j^{\mu} \zeta_j^{(t)} \right) - F_n \left(-\xi_i^{\mu} + \sum_{j \neq i} \xi_j^{\mu} \zeta_j^{(t)} \right) \right) \right] \\ &= \text{Sign} \left[\alpha \sum_{\mu} \left(F_n \left(\xi_i^{\mu} + \sum_{j \neq i} \xi_j^{\mu} \zeta_j^{(t)} \right) - F_n \left(-\xi_i^{\mu} + \sum_{j \neq i} \xi_j^{\mu} \zeta_j^{(t)} \right) \right) \right] \\ &= \text{Sign} \left[\sum_{\mu} \left(\alpha F_n \left(\xi_i^{\mu} + \sum_{j \neq i} \xi_j^{\mu} \zeta_j^{(t)} \right) - \alpha F_n \left(-\xi_i^{\mu} + \sum_{j \neq i} \xi_j^{\mu} \zeta_j^{(t)} \right) \right) \right] \end{aligned}$$

Moving α within the interaction function F_n requires constraints on the interaction function. We require that the sign of the difference remains the same. A stronger property would be to require that the interaction function is homogenous, meaning that the value of each interaction function evaluation remains the same after pulling α inside (up to possibly scaling α). This may exclude some nonhomogenous interaction functions from our proof, but these may be evaluated empirically for consistency if required. In general, proving that the sign of the difference remains constant is much more difficult than showing homogeneity, especially for more complex interaction functions. By Lemma 4.1.1 and 4.1.2, we know that the polynomial interaction function and rectified polynomial interaction function, two of the most common interaction functions, are homogenous. Assuming that the interaction function is homogenous:

$$\begin{aligned}
&= \text{Sign} \left[\sum_{\mu} \left(\alpha F_n \left(\xi_i^{\mu} + \sum_{j \neq i} \xi_j^{\mu} \zeta_j^{(t)} \right) - \alpha F_n \left(-\xi_i^{\mu} + \sum_{j \neq i} \xi_j^{\mu} \zeta_j^{(t)} \right) \right) \right] \\
&= \text{Sign} \left[\sum_{\mu} \left(F_n \left(\alpha' (\xi_i^{\mu} + \sum_{j \neq i} \xi_j^{\mu} \zeta_j^{(t)}) \right) - F_n \left(\alpha' (-\xi_i^{\mu} + \sum_{j \neq i} \xi_j^{\mu} \zeta_j^{(t)}) \right) \right) \right]
\end{aligned}$$

Since the scaled scaling factor α' is still arbitrary, we are free to select any (positive) value we like without changing the result. \square

Therefore, our modified network's update rule will give the same behavior as the original update rule in Equation 4. Our modified update rule is given by:

$$\zeta_i^{(t+1)} = \text{Sign} \left[\sum_{\mu} \left(F_n \left(\alpha (\xi_i^{\mu} + \sum_{j \neq i} \xi_j^{\mu} \zeta_j^{(t)}) \right) - F_n \left(\alpha (-\xi_i^{\mu} + \sum_{j \neq i} \xi_j^{\mu} \zeta_j^{(t)}) \right) \right) \right] \quad (12)$$

All that is left is to choose a value for the scaling factor α . As discussed, we suggest choosing $\alpha = \frac{1}{N}$, the inverse of the network dimension, such that the similarity scores are normalized between -1 and 1 , which nicely avoids floating point overflow. It may appear we are trading one floating point inaccuracy for another, as now our worst case would have small similarity scores (intermediate values close to 0) mapped even closer to 0 where again floating point numbers are inaccurate. However, the failure case here is to set the value to exactly 0.0 rather than “infinity” or “NaN”, and hence computation may continue albeit with reduced accuracy. Furthermore, once training has progressed slightly the memory vectors will likely be quite similar to the data, avoiding this problem. Finally, we could further tune the scaling factor if numerical instability is still a concern, as we have shown a general scaling factor is admissible. In practice, we found this was not required.

4.3 Learning in the Modern Hopfield Network

Reasoning about the learning rule (Equation 8) is slightly trickier than the update rule. We must ensure the network learning remains consistent rather than just the sign of an energy difference. Furthermore, there is already a scaling factor β present. We will show that we can pull the scaling factor within the interaction function and keep its intended behavior of shifting the argument of the tanh function, and hence that we can achieve the same calculation as the original network with our modifications. The argument here is largely the same as in Section 4.2, including the requirement for homogeneity of the interaction function, although in our tests all interaction functions trained to completion (including the non-homogenous leaky rectified polynomial interaction function).

Theorem 4.3.1. *The behavior of the modern Hopfield network learning rule (Equation 8) is unchanged when moving the scaling factor β inside the interaction function evaluations, up to adjusting the scaling factor.*

Proof. Equation 8 defines a loss function over which a gradient descent is applied to update the memory vectors ξ . To show this gradient descent is unchanged by moving the scaling factor β inside the the interaction function evaluations, we focus on the “predicted” neuron value $C_{a,i}$ and show the following equality:

$$\begin{aligned} C_{a,i} &= \tanh \left[\beta' \sum_{\mu} \left(F_n \left(\xi_i^{\mu} + \sum_{j \neq i} \xi_j^{\mu} \zeta_{a,j}^{(t)} \right) - F_n \left(-\xi_i^{\mu} + \sum_{j \neq i} \xi_j^{\mu} \zeta_{a,j}^{(t)} \right) \right) \right] \\ &= \tanh \left[\sum_{\mu} \left(F_n \left(\beta(\xi_i^{\mu} + \sum_{j \neq i} \xi_j^{\mu} \zeta_{a,j}^{(t)}) \right) - F_n \left(\beta(-\xi_i^{\mu} + \sum_{j \neq i} \xi_j^{\mu} \zeta_{a,j}^{(t)}) \right) \right) \right] \end{aligned}$$

Starting with the original “predicted” neuron value $C_{a,i}$ from Equation 8, we apply the same algebra as in Theorem 4.2.1 to take the scaling factor β' inside. Note this also requires the homogeneity of the interaction function, and may scale the scaling factor β , but will ensure the argument to the tanh function remains the same. Since the argument to the tanh function has not changed, the learning behavior is identical. \square

Therefore, our modified learning rule has the form:

$$C_{a,i} = \tanh \left[\sum_{\mu} \left(F_n \left(\beta(\xi_i^{\mu} + \sum_{j \neq i} \xi_j^{\mu} \zeta_{a,j}^{(t)}) \right) - F_n \left(\beta(-\xi_i^{\mu} + \sum_{j \neq i} \xi_j^{\mu} \zeta_{a,j}^{(t)}) \right) \right) \right] \quad (13)$$

Of course, this may change the *scale* of the scaling factor β , but will retain the same behavior as the unmodified network. Krotov and Hopfield suggest a value of $\beta = \frac{1}{T^n}$. We suggest a modified value of $\beta = \frac{1}{NT}$. Since interaction functions of interest have a degree of homogeneity equal to the interaction vertex n , shifting the scaling factor inside is effectively equivalent to taking the exponent of $\frac{1}{n}$, so we can remove the exponent from Krotov and Hopfield’s suggestion. Furthermore, as in Section 4.2 we suggest normalizing the similarity score by the network dimension to be bounded between -1 and 1 . It may seem alarming that we suggest massively lowering the similarity score in this equation, as it may affect the argument passed to the tanh function and hence the magnitude of the gradients used in learning, but we can always simply rescale β using the temperature to increase this value again if required. However, the default behavior of the network now results in rapidly

shrinking intermediate values during training, rather than exploding values that are often unrecoverable. By tuning β we can shift the argument to tanh just as we could in the unmodified network while still avoiding floating point overflow.

4.4 On the Exponential Interaction Function

The modern Hopfield network has been generalized further using an exponential interaction function (Demircigil et al., 2017). Another modification of the exponential interaction function has been used to allow for continuous states and an exponential capacity (Ramsauer et al., 2021). This interaction function has been analyzed in depth and linked to the attention mechanism in transformer architectures (Vaswani et al., 2017). For completion, we discuss our proposed modifications to the new, wildly popular interaction function:

$$F(x) = e^x, \tag{14}$$

Clearly, the exponential interaction function is not homogenous, as

$$\begin{aligned} F(ax) &= e^{ax} \\ &= e^a e^x \\ &= e^a F(x) \end{aligned}$$

Since the constant a does not have the form a^k when pulled out of the function, the exponential function is not homogenous. However, the sign of the difference between two exponentials can be analyzed, unlike the general case:

$$\begin{aligned} \text{Sign}[k(F(x) - F(y))] &= \text{Sign}[k(e^x - e^y)] \\ &= \text{Sign}[ae^x - ae^y] \\ &= \text{Sign}\left[e^{\log(a)}e^x - e^{\log(a)}e^y\right] \\ &= \text{Sign}\left[e^{\log(a)x} - e^{\log(a)y}\right] \end{aligned}$$

And so the behavior of the modern Hopfield network using the exponential interaction function would be unchanged by normalizing the similarity scores before taking the exponential, preventing computation of large floating point numbers. This may help stabilize the continuous modern Hopfield network and improve integrations in deep learning architectures.

5 Hyperparameter Tuning

The original modern Hopfield network suffered from very strict hyperparameter requirements. Furthermore, changing the value of the interaction vertex would significantly change

the hyperparameters that would train the model well. We find that normalizing the similarity scores in the learning rule (Equation 13) removed the dependence on the interaction vertex, meaning we can reuse the same hyperparameters for a task even as we change the interaction vertex.

We focus on the most important hyperparameters for learning: the initial learning rate and temperature. Other hyperparameters are kept constant throughout the following experiments. Specifically, we used a learning rate decay of 0.999 per epoch, a momentum of 0.0, and an error exponent of $m = 1.0$. We found similar results using a decay rate of 1.0 and higher values for momentum but kept the learning process as simple as possible to avoid additional complexities. We also note that we did not require changing the error exponent, which Krotov and Hopfield note was useful in learning higher interaction vertices. This may suggest that we could remove the need for tuning this hyperparameter when our modifications are used.

Our experiments created a network with a particular set of hyperparameters – the fixed ones above as well as a variable interaction vertex, initial learning rate, and temperature. The network is trained on 20 randomly generated bipolar vectors of dimension 100. Even for the lowest interaction vertex $n = 2$, this task is perfectly learnable. Larger dimensions and other dataset sizes were tested with similar results. After training, we probe the network with the learned states; if the learned states are unstable the network fails as an autoassociative memory. If the learned states only move a small amount, that may be an acceptable performance. We measure the average distance from the final states to the learned states, for which a lower value is better. We repeat the experiment five times for each combination of hyperparameters.

5.1 Original Network Hyperparameter Results

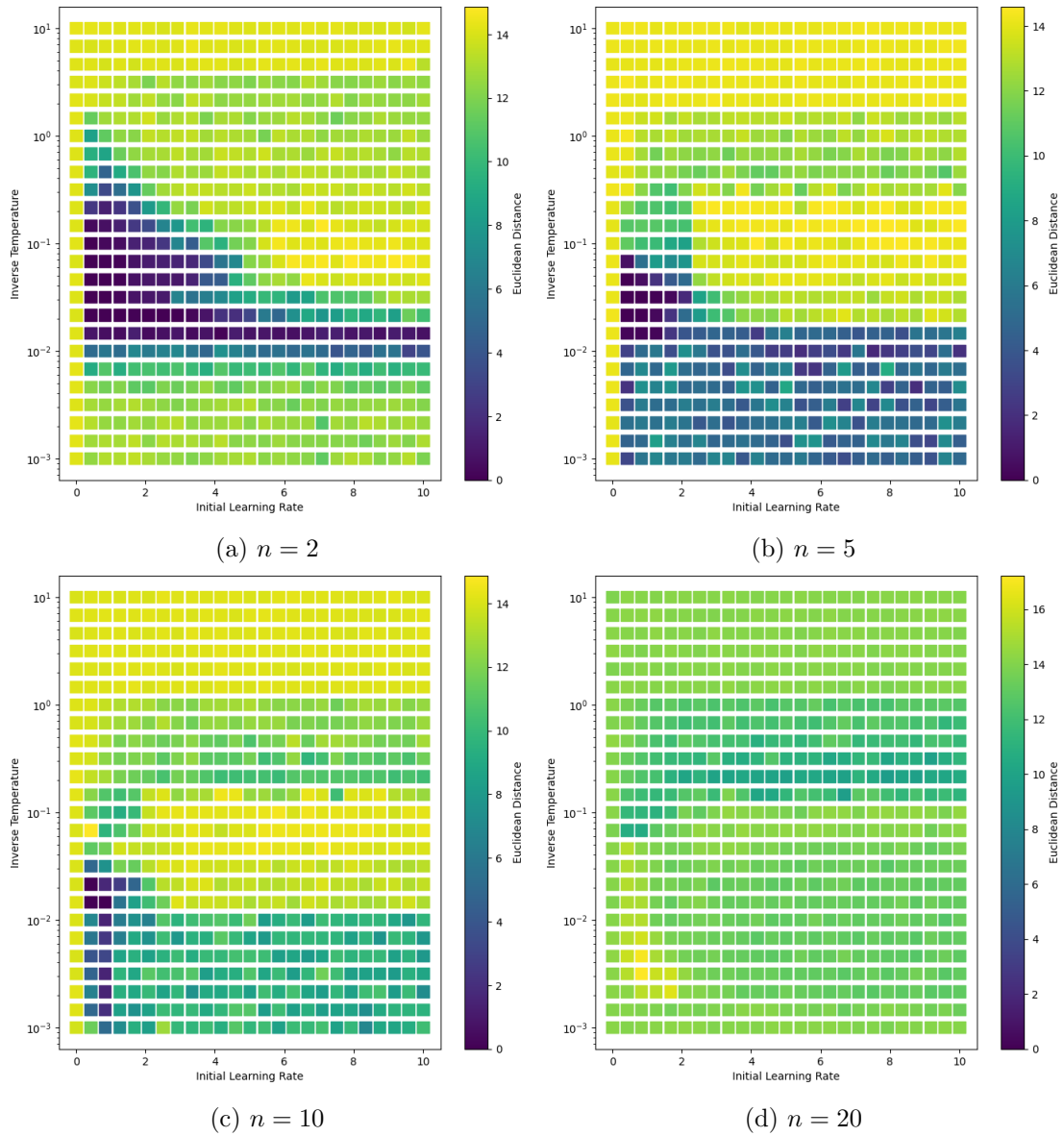


Figure 1: Coarse hyperparameter search space for the original network, measuring the Euclidean distance between learned states and relaxed states over various interaction vertices. Smaller distances correspond to better recall and hence better a better associative memory.

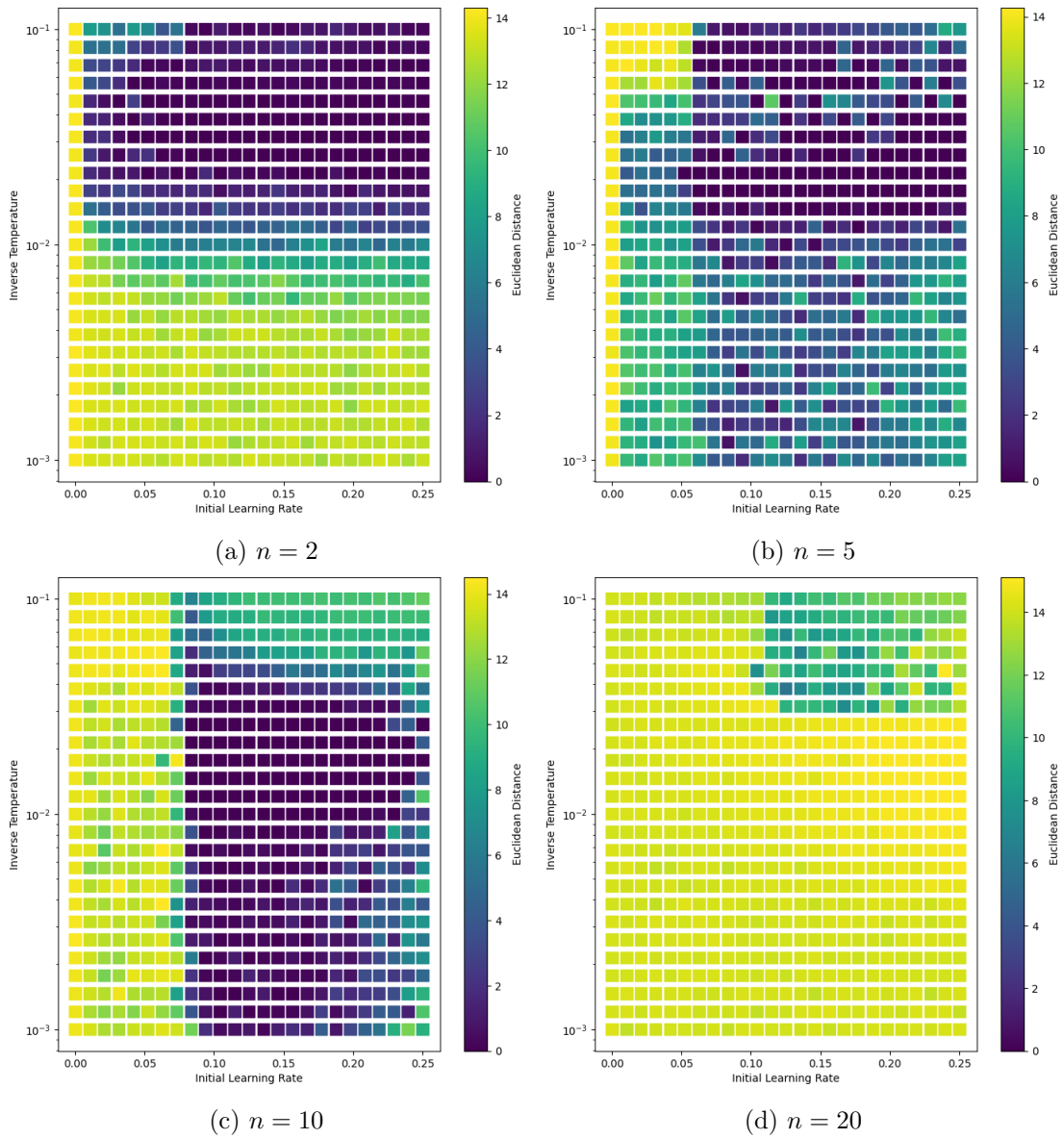


Figure 2: Fine hyperparameter search space for the original network, measuring the Euclidean distance between learned states and relaxed states over various interaction vertices. Smaller distances correspond to better recall and hence better a better associative memory.

Figure 1 shows the hyperparameters across networks with various interaction vertices. The color of the heat map shows how far the relaxed states are from the original learned states, with lower / darker values being better. The optimal region – that is, the combination of

hyperparameters that give low distances – is somewhere around $\frac{1}{T} \approx 10^{-2}$ and learning rate ≈ 0.5 but shifts considerably with the interaction vertex. We also find a significant increase in distance with the learning rate; higher learning rates tend to degrade network performance. At even modest interaction vertices, much less than what Krotov and Hopfield used ($n = 30$), we find the optimal region is fleeting enough to not appear in our grid search. It is tempting to claim that a finer grid search may reveal the region to persist. However, closer inspection of Figure 1d shows that not only has the optimal region vanished at this granularity, but the same region has *increased* the distance measure compared to its surroundings. Even if the optimal region exists and is very small, it is apparently surrounded by an increasingly suboptimal region. This behavior is troublesome and makes working with the network difficult.

Note we have avoided floating point overflow by engineering our experiments to remain within the bounds of a double. In general, this network would fail to train for larger interaction vertices or data dimensions. However, the performance degradation seen at larger interaction vertices in Figure 1 is not due to floating point overflow.

5.2 Modified Network Hyperparameter Results

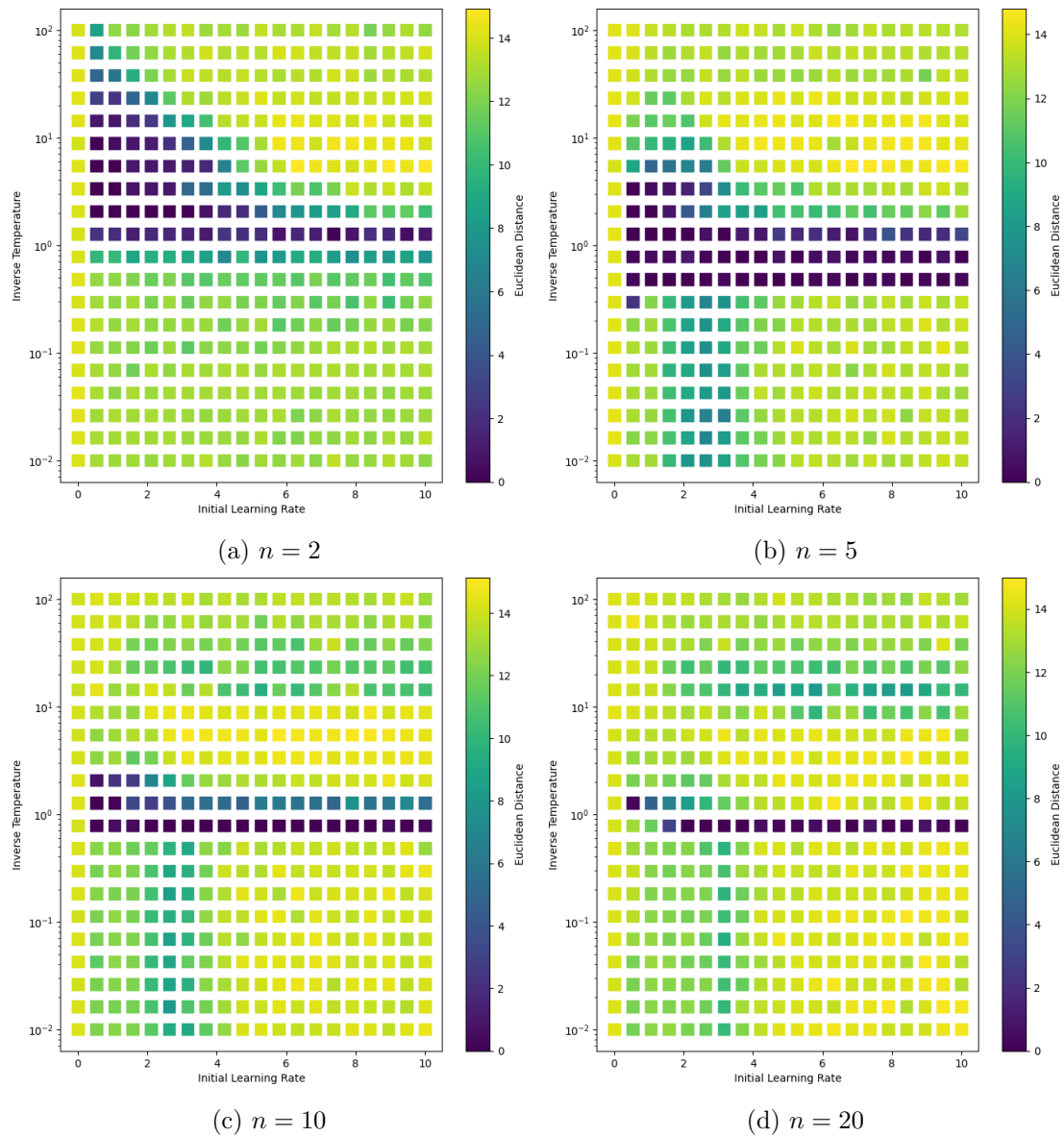


Figure 3: Coarse hyperparameter search space for the modified network, measuring the Euclidean distance between learned states and relaxed states over various interaction vertices. Smaller distances correspond to better recall and hence better associative memory.

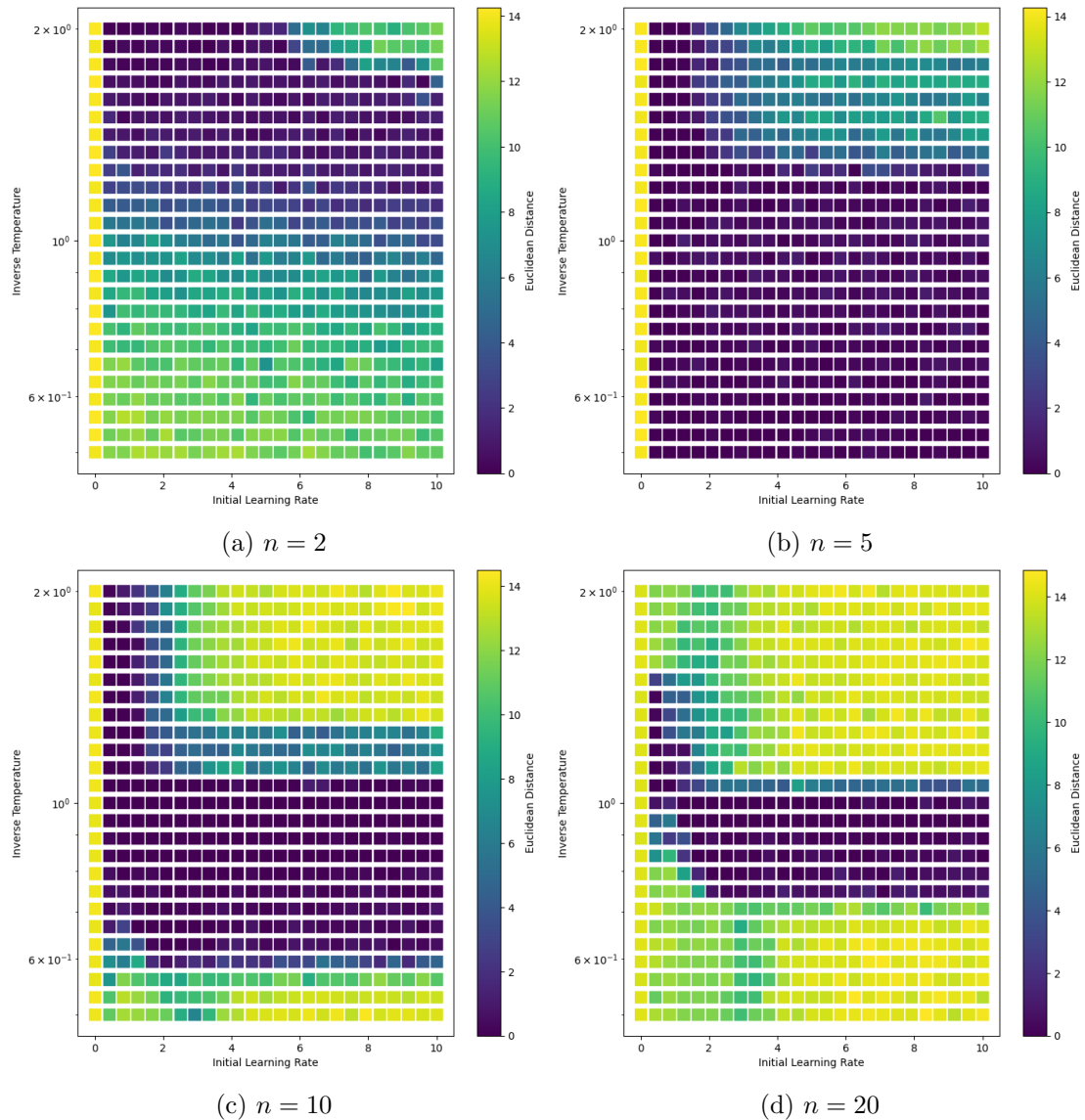


Figure 4: Fine hyperparameter search space for the modified network, measuring the Euclidean distance between learned states and relaxed states over various interaction vertices. Smaller distances correspond to better recall and hence better a better associative memory.

Figure 3 shows the same hyperparameter search for our modified network. Note we have shifted the scale of the inverse temperature as discussed in Section 4. As in Figure 1 we find the optimal region shifts slightly for small interaction vertices ($n \leq 5$) but unlike the original network we find the region stabilizes and remains substantial for large interaction

vertices. Figure 4 shows a finer grid search over the region of interest, showing the optimal region stabilizes around $\frac{1}{T} \approx 9 \cdot 10^{-1}$. The optimal region also extends to much larger initial learning rates than it does in the original network. Most notably, we find that the optimal region’s position remains stable and size remains large across many values of the interaction vertex for the same network dimension.

All of our results can be found in Appendix A. In particular, Appendix A.3 shows our results for interaction vertices up to 100; far above any interaction vertices documented in other literature.

6 Conclusion

In this work, we have investigated the technical details of the modern Hopfield network and its implementation. We note that the original network specification leads to floating point imprecision and overflow when calculating intermediate values for both update and learning. We provide details on when this imprecision occurs and show the conditions are more likely when the interaction vertex is large based on the feature-to-prototype transition observed (Krotov and Hopfield, 2016). We propose a modification to the network implementation that prevents the floating point issues. We prove our modifications do not alter the network behavior for update or learning. Our proof relies on the interaction function being homogenous, however this property is stronger than is required, and we find empirically that some nonhomogenous functions also give well-behaved modern Hopfield networks. We then show our modified network has optimal hyperparameter regions that do not shift based on the choice of interaction vertex. This makes working with the modern Hopfield network much easier, as experiments on a dataset do not need to search across a potentially large hyperparameter space for each change in the interaction vertex. We also find several hyperparameters do not need tuning in our experiments, hinting at a potentially simpler network that is easier to tune and interpret.

References

- [1] Nicholas Alonso and Jeffrey L. Krichmar. “A sparse quantized hopfield network for online-continual memory”. en. In: *Nature Communications* 15.1 (May 2024). Publisher: Nature Publishing Group, p. 3722. ISSN: 2041-1723. DOI: 10.1038/s41467-024-46976-4.
- [2] Jimmy Lei Ba, Jamie Ryan Kiros, and Geoffrey E. Hinton. *Layer Normalization*. arXiv:1607.06450 [cs, stat]. July 2016. DOI: 10.48550/arXiv.1607.06450.
- [3] Mete Demircigil et al. “On a Model of Associative Memory with Huge Storage Capacity”. en. In: *Journal of Statistical Physics* 168.2 (July 2017), pp. 288–299. ISSN: 0022-4715, 1572-9613. DOI: 10.1007/s10955-017-1806-y.

- [4] D. O. Hebb. *The organization of behavior; a neuropsychological theory*. The organization of behavior; a neuropsychological theory. Pages: xix, 335. Oxford, England: Wiley, 1949.
- [5] John A. Hertz. *Introduction To The Theory Of Neural Computation*. Boca Raton: CRC Press, 1991. ISBN: 978-0-429-49966-1. DOI: 10.1201/9780429499661.
- [6] J J Hopfield. “Neural networks and physical systems with emergent collective computational abilities.” In: *Proceedings of the National Academy of Sciences* 79.8 (Apr. 1982). Publisher: Proceedings of the National Academy of Sciences, pp. 2554–2558. DOI: 10.1073/pnas.79.8.2554.
- [7] J. J. Hopfield. “Neurons with Graded Response Have Collective Computational Properties like Those of Two-State Neurons”. In: *Proceedings of the National Academy of Sciences of the United States of America* 81.10 (1984). Publisher: National Academy of Sciences, pp. 3088–3092. ISSN: 0027-8424.
- [8] J. J. Hopfield and D. W. Tank. ““Neural” computation of decisions in optimization problems”. en. In: *Biological Cybernetics* 52.3 (July 1985), pp. 141–152. ISSN: 1432-0770. DOI: 10.1007/BF00339943.
- [9] “IEEE Standard for Floating-Point Arithmetic”. In: *IEEE Std 754-2019 (Revision of IEEE 754-2008)* (July 2019). Conference Name: IEEE Std 754-2019 (Revision of IEEE 754-2008), pp. 1–84. DOI: 10.1109/IEEESTD.2019.8766229.
- [10] Sergey Ioffe and Christian Szegedy. *Batch Normalization: Accelerating Deep Network Training by Reducing Internal Covariate Shift*. arXiv:1502.03167 [cs]. Mar. 2015. DOI: 10.48550/arXiv.1502.03167.
- [11] Dmitry Krotov and John Hopfield. “Dense Associative Memory Is Robust to Adversarial Inputs”. In: *Neural Computation* 30.12 (Dec. 2018), pp. 3151–3167. ISSN: 0899-7667. DOI: 10.1162/neco_a_01143.
- [12] Dmitry Krotov and John Hopfield. *Large Associative Memory Problem in Neurobiology and Machine Learning*. arXiv:2008.06996 [cond-mat, q-bio, stat]. Apr. 2021. DOI: 10.48550/arXiv.2008.06996.
- [13] Dmitry Krotov and John J. Hopfield. “Dense Associative Memory for Pattern Recognition”. In: *Advances in Neural Information Processing Systems*. Vol. 29. Curran Associates, Inc., 2016.
- [14] Yuchen Liang, Dmitry Krotov, and Mohammed J. Zaki. “Modern Hopfield Networks for graph embedding”. English. In: *Frontiers in Big Data* 5 (Nov. 2022). Publisher: Frontiers. ISSN: 2624-909X. DOI: 10.3389/fdata.2022.1044709.
- [15] R. McEliece et al. “The capacity of the Hopfield associative memory”. In: *IEEE Transactions on Information Theory* 33.4 (July 1987). Conference Name: IEEE Transactions on Information Theory, pp. 461–482. ISSN: 1557-9654. DOI: 10.1109/TIT.1987.1057328.

- [16] Beren Millidge et al. “Universal Hopfield Networks: A General Framework for Single-Shot Associative Memory Models”. en. In: *Proceedings of the 39th International Conference on Machine Learning*. ISSN: 2640-3498. PMLR, June 2022, pp. 15561–15583.
- [17] Hubert Ramsauer et al. *Hopfield Networks is All You Need*. arXiv:2008.02217 [cs, stat]. Apr. 2021. DOI: 10.48550/arXiv.2008.02217.
- [18] Philipp Seidl et al. *Modern Hopfield Networks for Few- and Zero-Shot Reaction Template Prediction*. arXiv:2104.03279 [cs, q-bio, stat]. June 2021. DOI: 10.48550/arXiv.2104.03279.
- [19] Ashish Vaswani et al. “Attention is all you need”. In: *Proceedings of the 31st International Conference on Neural Information Processing Systems*. NIPS’17. Red Hook, NY, USA: Curran Associates Inc., Dec. 2017, pp. 6000–6010. ISBN: 978-1-5108-6096-4. (Visited on 07/29/2024).

A Full Results of Hyperparameter Searches

A.1 Original Network, Dimension 100

These results are from the original network, have dimension 100, and train on 20 learned states.

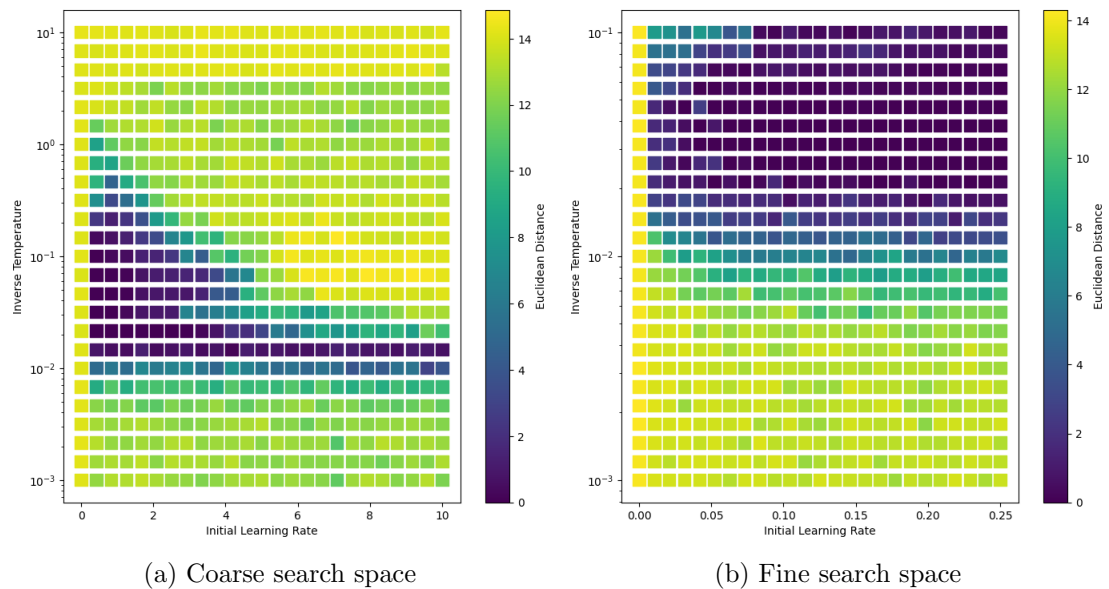
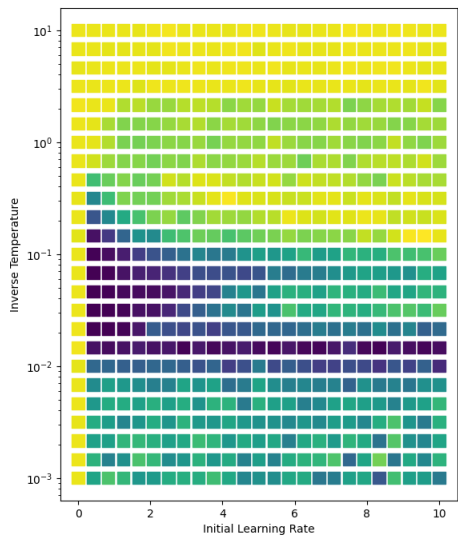
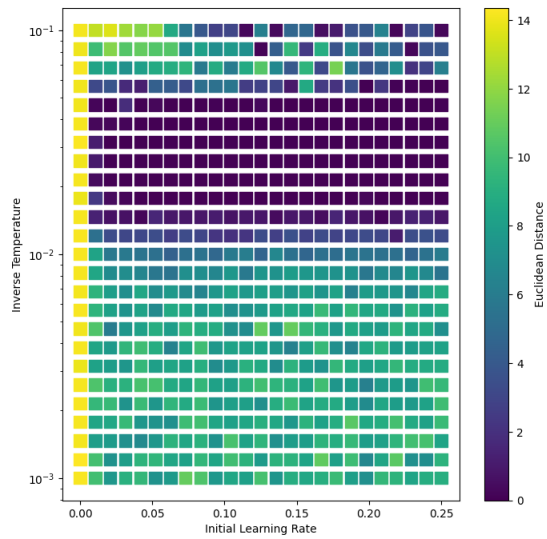


Figure 5: Hyperparameter search space for $n = 2$

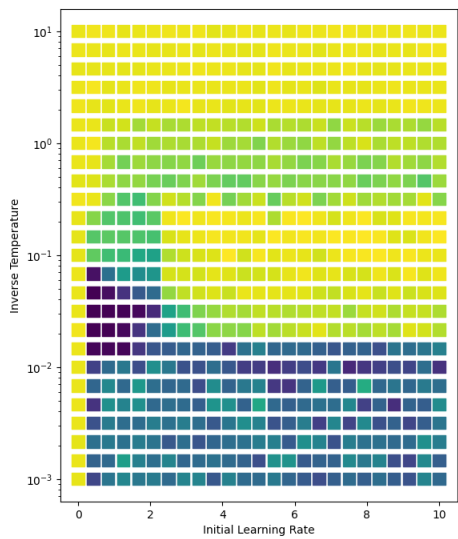


(a) Coarse search space

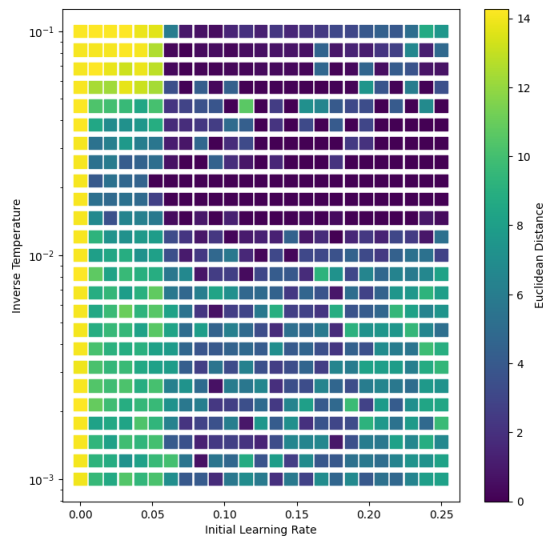


(b) Fine search space

Figure 6: Hyperparameter search space for $n = 3$

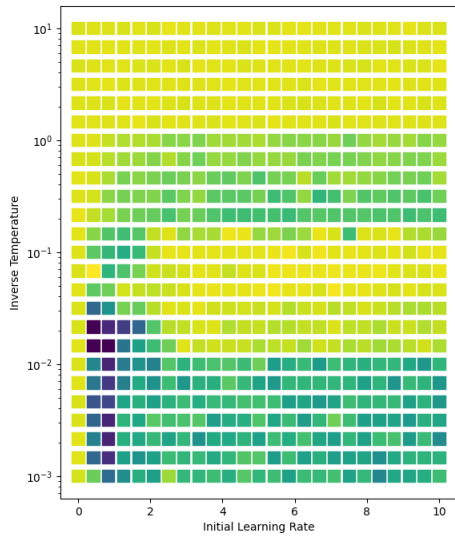


(a) Coarse search space

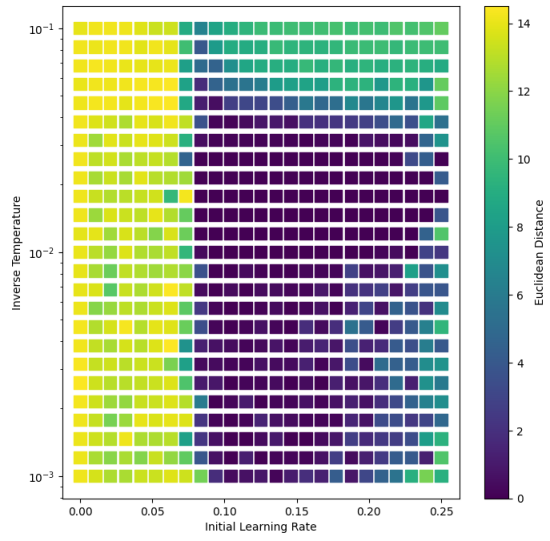


(b) Fine search space

Figure 7: Hyperparameter search space for $n = 5$

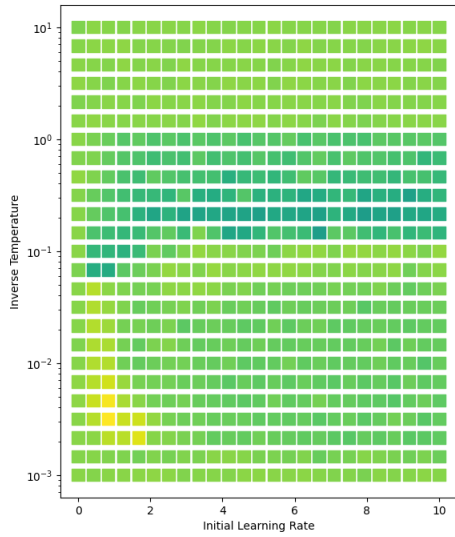


(a) Coarse search space

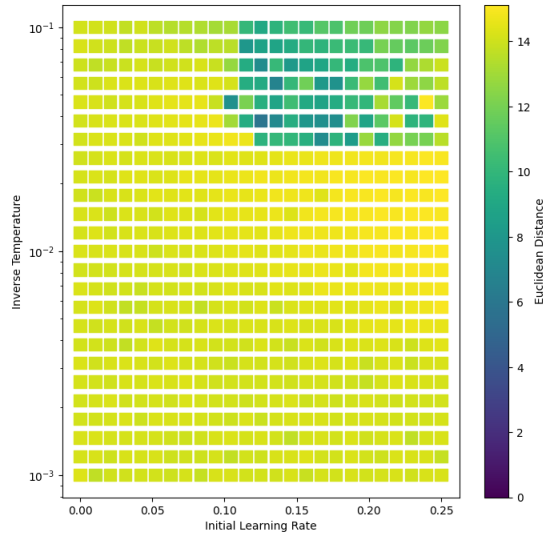


(b) Fine search space

Figure 8: Hyperparameter search space for $n = 10$

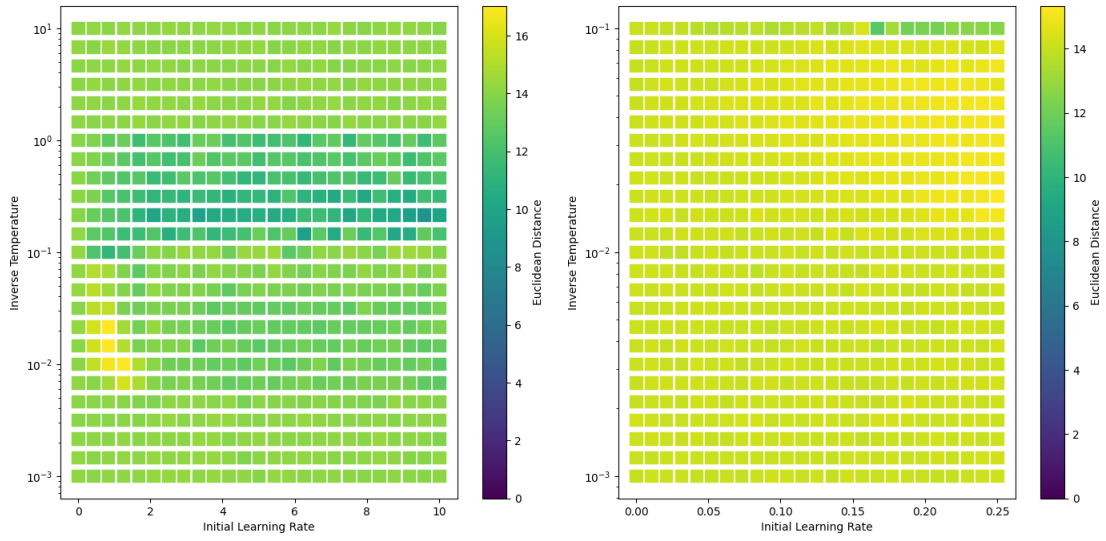


(a) Coarse search space



(b) Fine search space

Figure 9: Hyperparameter search space for $n = 20$



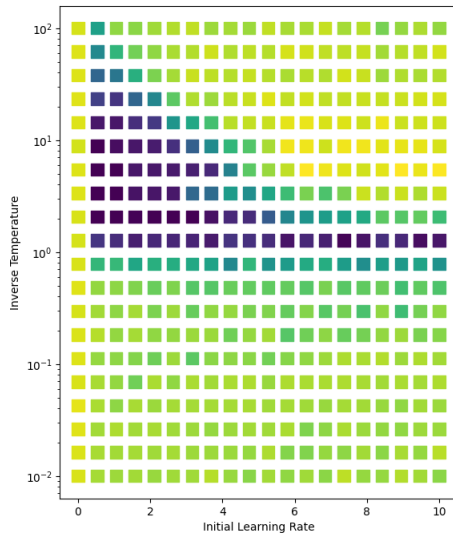
(a) Coarse search space

(b) Fine search space

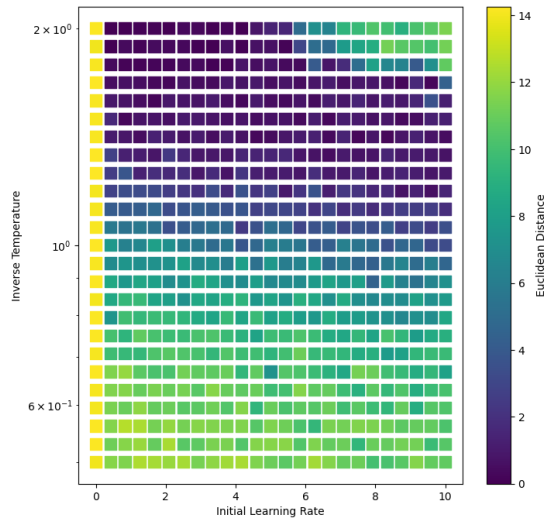
Figure 10: Hyperparameter search space for $n = 30$

A.2 Modified Network, Dimension 100

These results are from our modified network, have dimension 100, and train on 20 learned states.

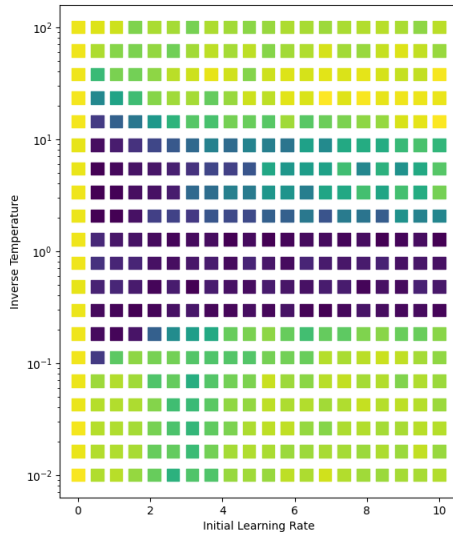


(a) Coarse search space

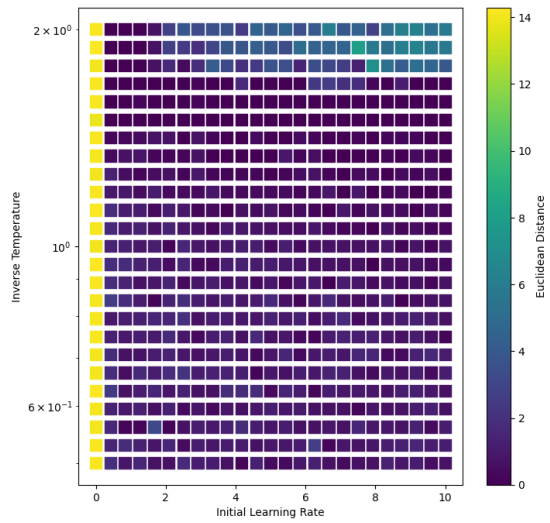


(b) Fine search space

Figure 11: Hyperparameter search space for $n = 2$

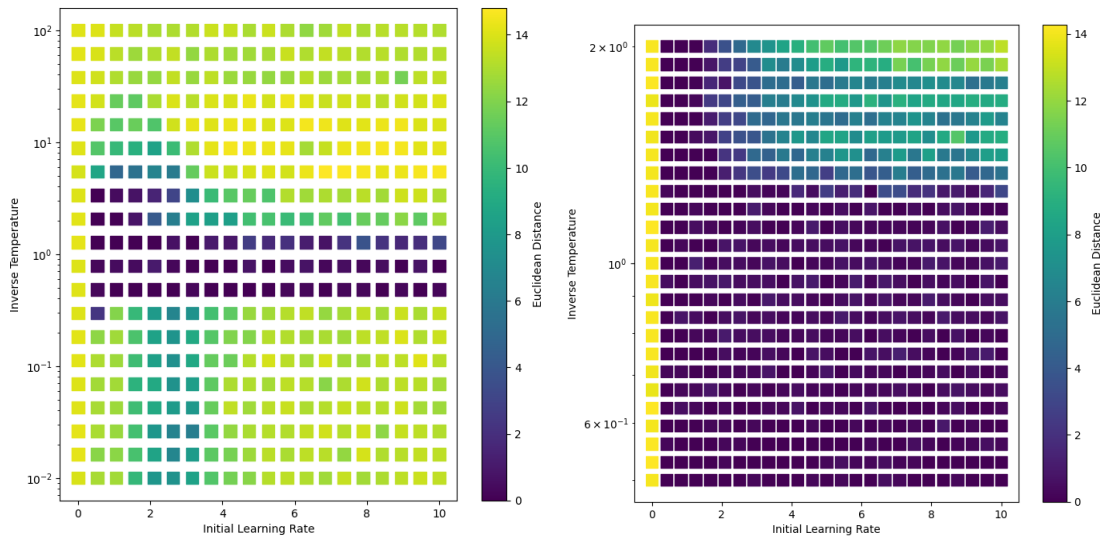


(a) Coarse search space



(b) Fine search space

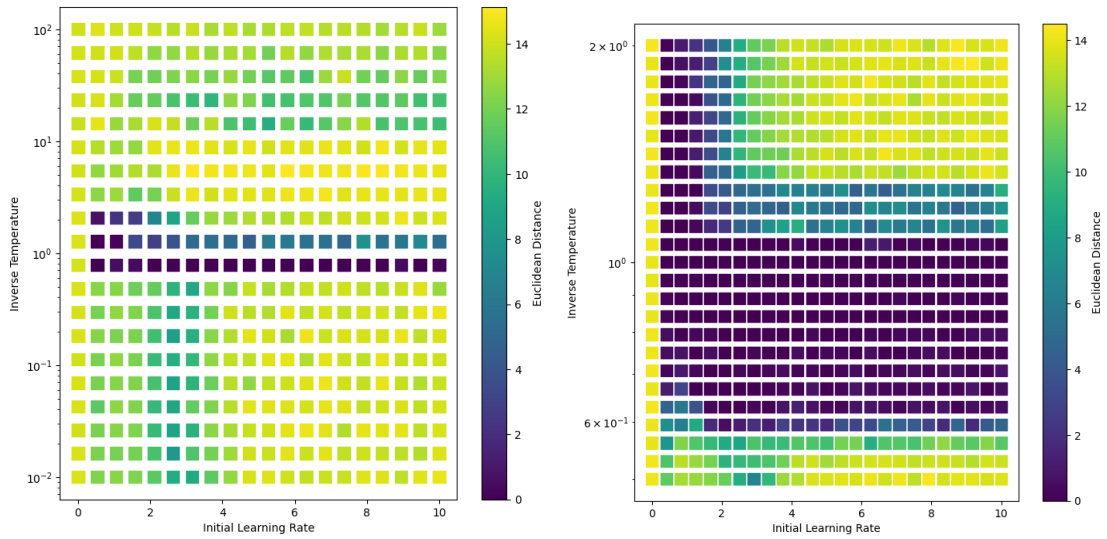
Figure 12: Hyperparameter search space for $n = 3$



(a) Coarse search space

(b) Fine search space

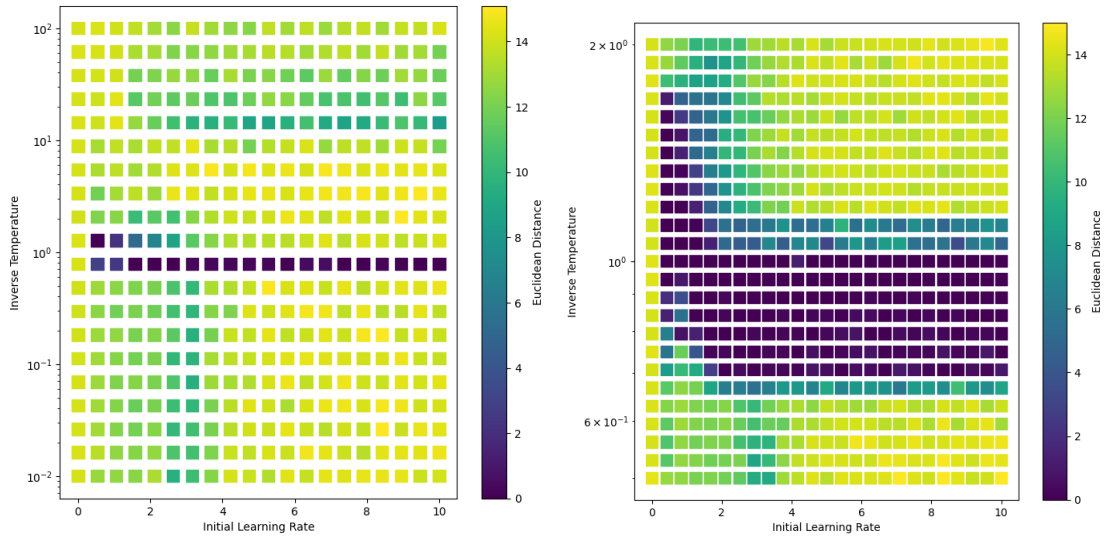
Figure 13: Hyperparameter search space for $n = 5$



(a) Coarse search space

(b) Fine search space

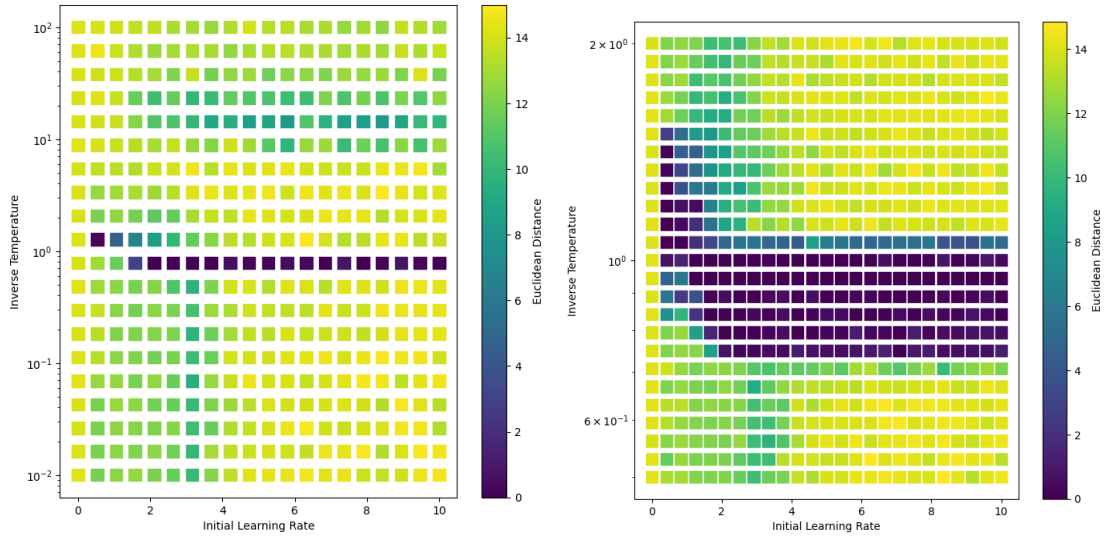
Figure 14: Hyperparameter search space for $n = 10$



(a) Coarse search space

(b) Fine search space

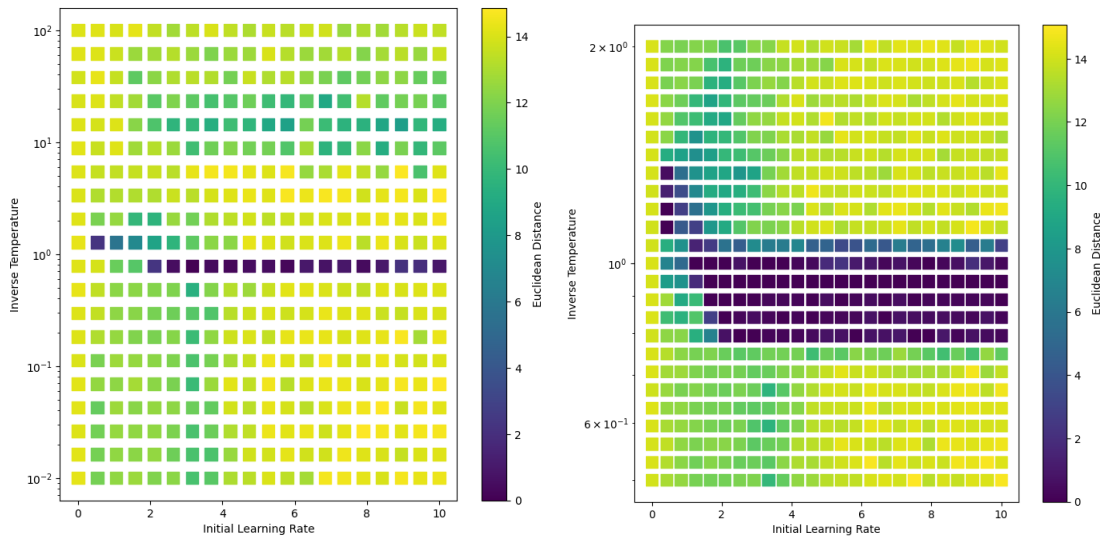
Figure 15: Hyperparameter search space for $n = 15$



(a) Coarse search space

(b) Fine search space

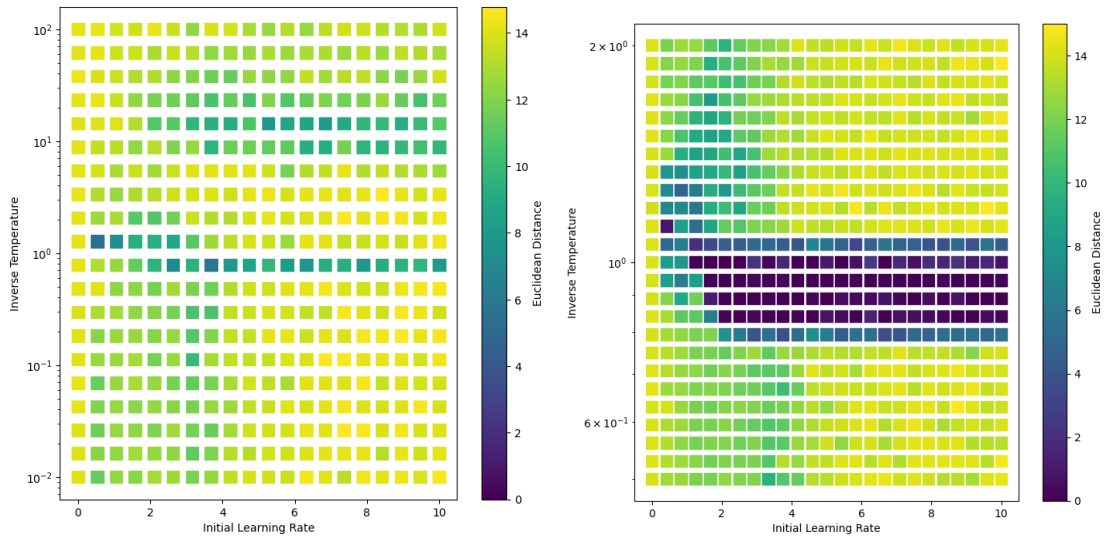
Figure 16: Hyperparameter search space for $n = 20$



(a) Coarse search space

(b) Fine search space

Figure 17: Hyperparameter search space for $n = 25$



(a) Coarse search space

(b) Fine search space

Figure 18: Hyperparameter search space for $n = 30$

A.3 Modified Network, Dimension 100, Large n

These results continue with the same network and setup from Appendix A.2 but with much larger interaction vertices than were possible with the original network. We also present only the tight grid search results, as the coarse grid search did not capture the optimal region well.

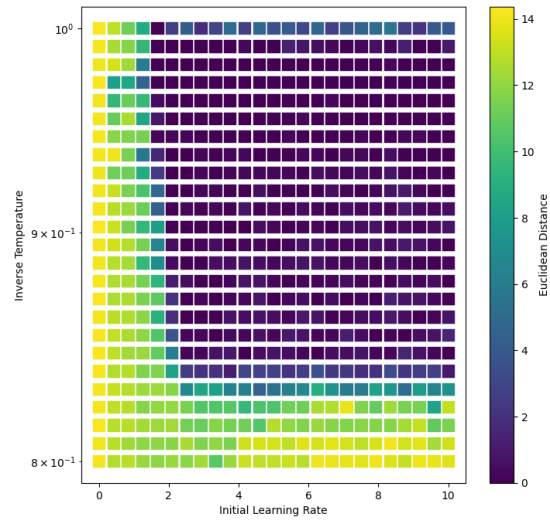


Figure 19: Hyperparameter search space for $n = 40$

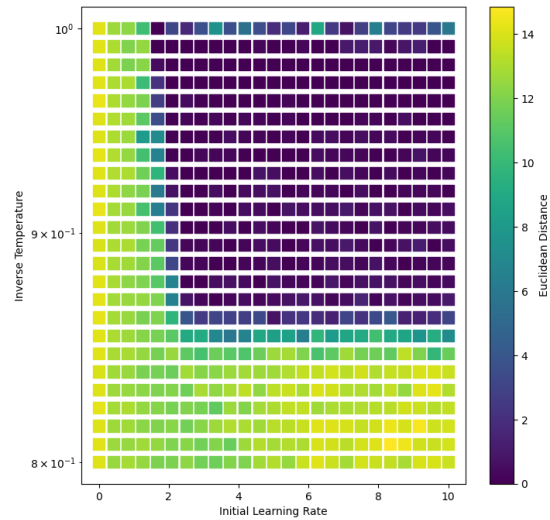


Figure 20: Hyperparameter search space for $n = 50$

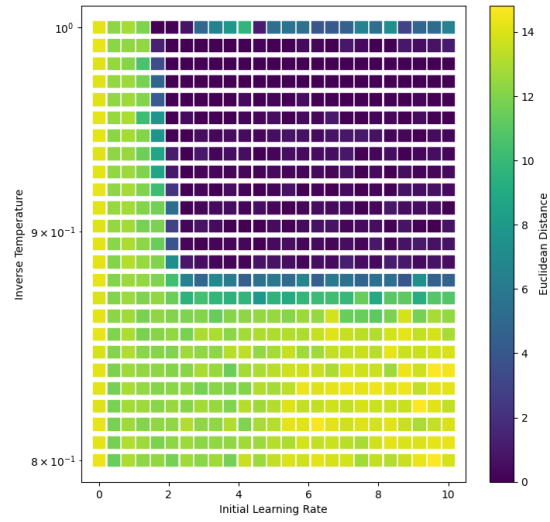


Figure 21: Hyperparameter search space for $n = 60$

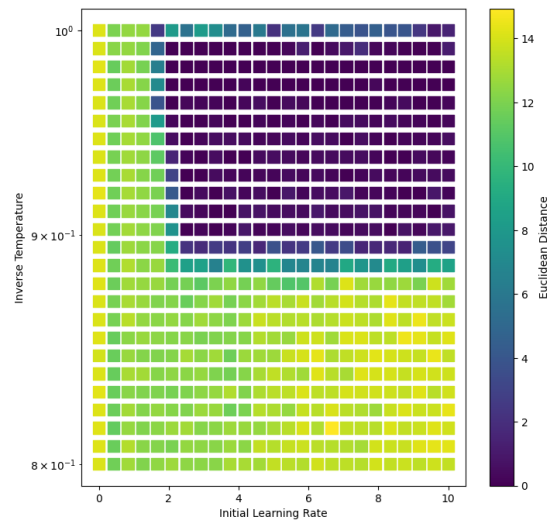


Figure 22: Hyperparameter search space for $n = 70$

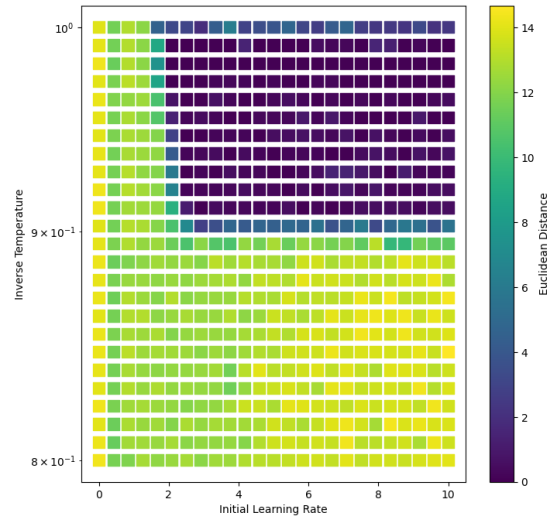


Figure 23: Hyperparameter search space for $n = 80$

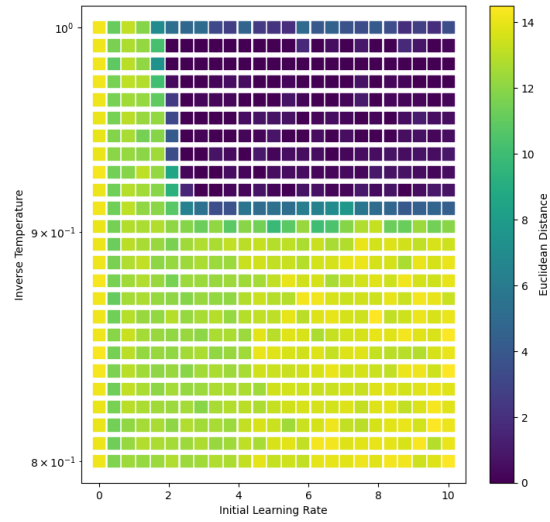


Figure 24: Hyperparameter search space for $n = 90$

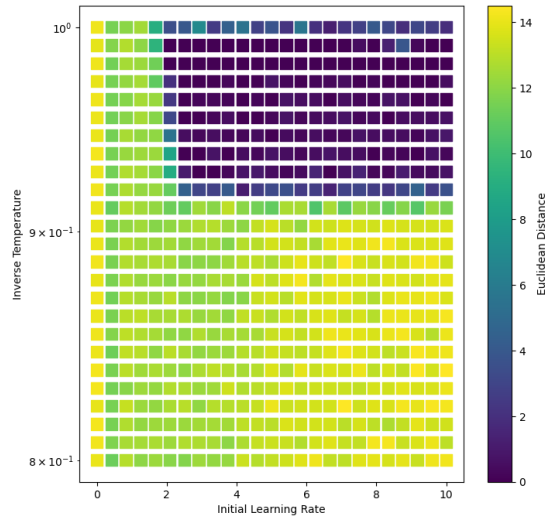


Figure 25: Hyperparameter search space for $n = 100$

A.4 Modified Network, Dimension 250

These results are from our modified network, have dimension 250, and train on 30 learned states.

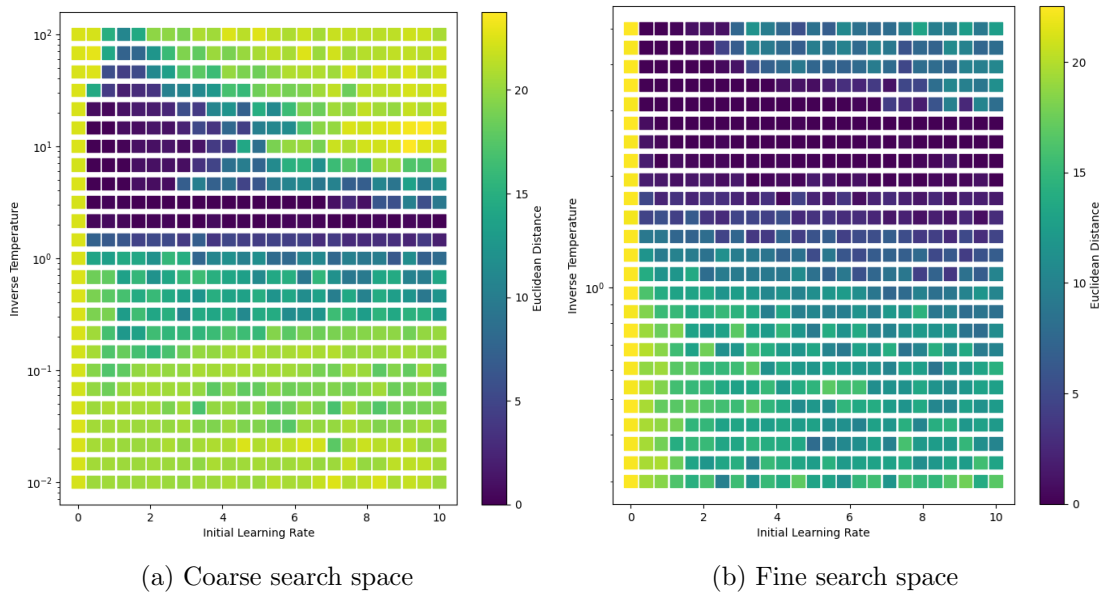
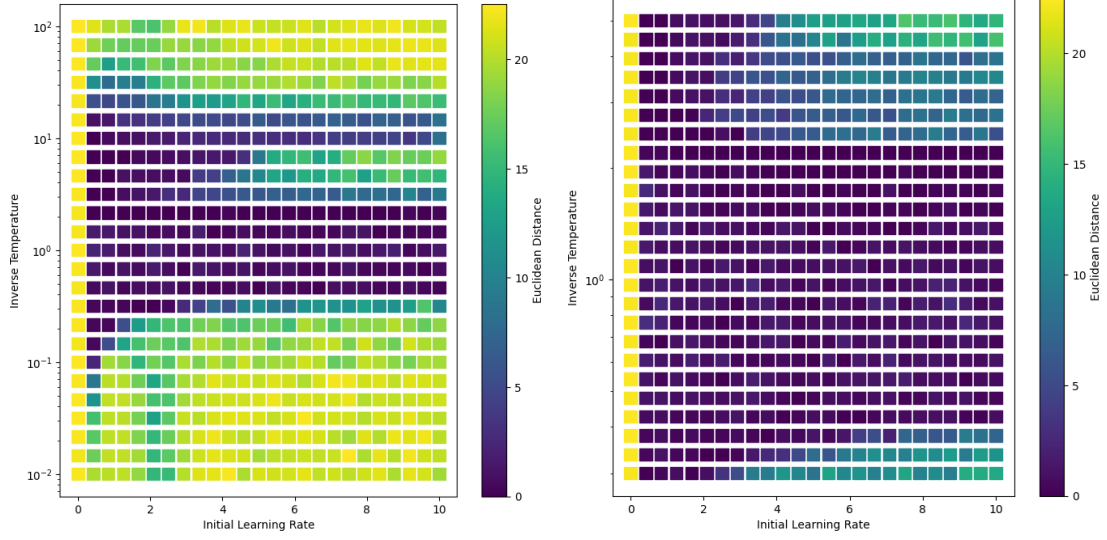


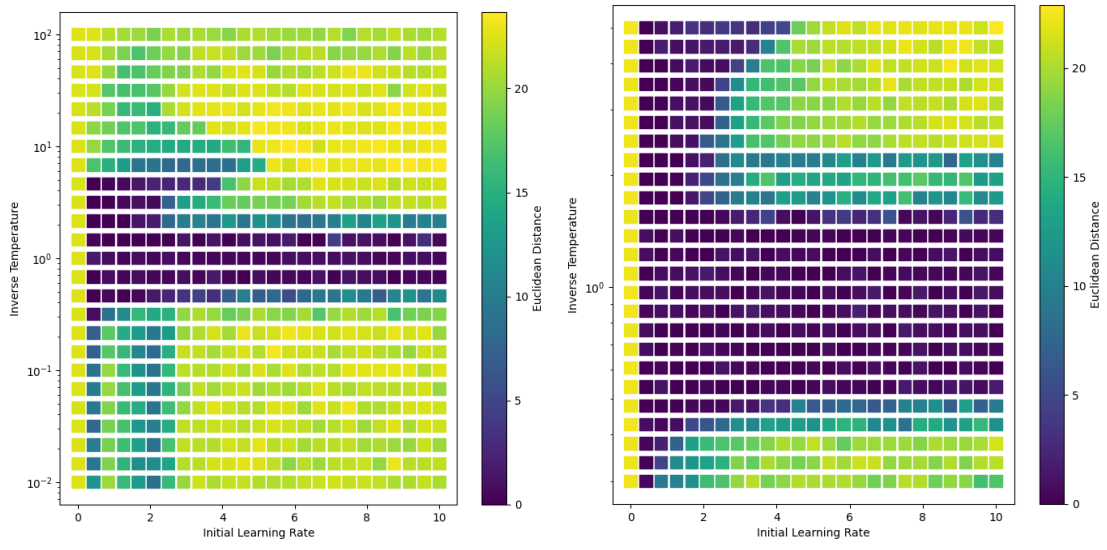
Figure 26: Hyperparameter search space for $n = 2$



(a) Coarse search space

(b) Fine search space

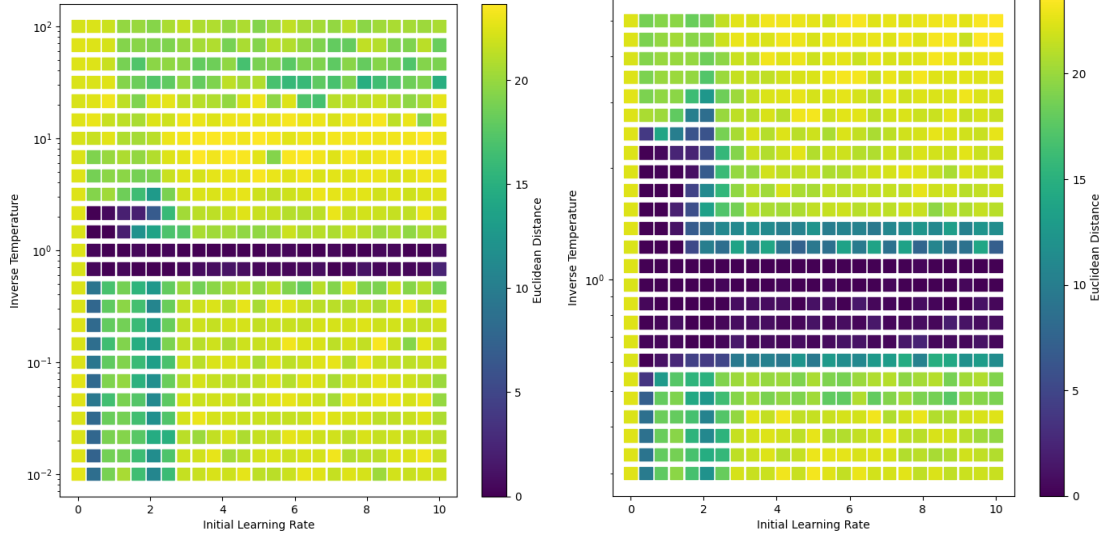
Figure 27: Hyperparameter search space for $n = 3$



(a) Coarse search space

(b) Fine search space

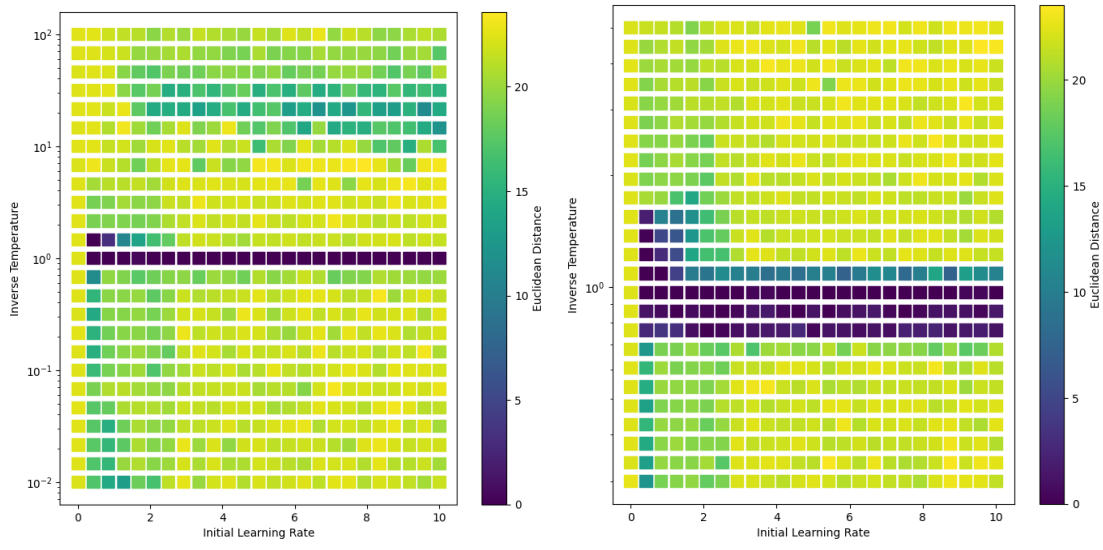
Figure 28: Hyperparameter search space for $n = 5$



(a) Coarse search space

(b) Fine search space

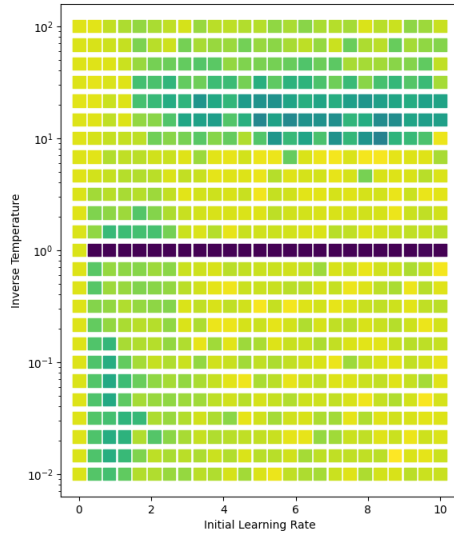
Figure 29: Hyperparameter search space for $n = 10$



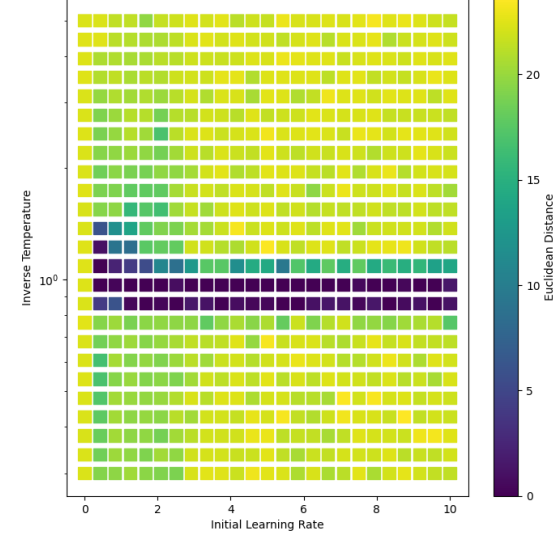
(a) Coarse search space

(b) Fine search space

Figure 30: Hyperparameter search space for $n = 20$



(a) Coarse search space



(b) Fine search space

Figure 31: Hyperparameter search space for $n = 30$